

## Dispersion of Gold in Polycarbonate by Vapor-Induced Crystallization

Krzysztof K. K. Koziol,<sup>†,§</sup> Kai Dolgner,<sup>†</sup> Nobuo Tsuboi,<sup>‡</sup> Jan Kruse,<sup>†</sup>  
Vladimir Zaporozhchenko,<sup>†</sup> Shigehito Deki,<sup>‡</sup> and Franz Faupel<sup>\*,†</sup>

Technische Fakultät der Christian-Albrechts-Universität Kiel, Lehrstuhl für Materialverbunde, Kaiserstr. 2, D-24143 Kiel, Germany, and Department of Chemical Science and Engineering, Kobe University, Rokkodai-cho, Nado-ku, Kobe 657-8501, Japan

Received August 22, 2003; Revised Manuscript Received November 27, 2003

**ABSTRACT:** It has been demonstrated that dispersion of noble metal nanoparticles in an organic matrix can be achieved by crystallization of amorphous low-molecular-weight nylon-11 in a process called relaxative autodispersion. In the present paper we report the dispersion of Au by acetone vapor-induced crystallization of amorphous polycarbonate films. Crystallization kinetics were examined with infrared spectroscopy. Au dispersion was detected with X-ray photoelectron spectroscopy in conjunction with ion-beam depth profiling and cross-sectional transmission electron microscopy. While vapor sorption in films of some micrometers thickness occurs within minutes at room temperature, crystallization and Au dispersion take place on a time scale of hours. Crystallization gives rise to a strong enhancement of surface roughness measured by atomic force microscopy. The present approach of metal dispersion is not restricted to low-molecular-weight polymers. A model for the dispersion process is proposed.

## Introduction

Recently, there is much interest in composites consisting of metallic nanoparticles in organic matrices because of their interesting optical,<sup>1</sup> electrical,<sup>2</sup> thermodynamic,<sup>3</sup> catalytic,<sup>4</sup> and magnetic properties.<sup>5</sup> Various techniques have been developed to produce a fine dispersion of metals in an organic matrix. These include reduction of a metal salt in a polymer solution<sup>6</sup> and metal evaporation upon plasma polymerization<sup>7</sup> as well as coevaporation<sup>8,9</sup> and co-sputtering of the organic and metallic components.<sup>10</sup> A particularly striking process termed relaxative autodispersion has been developed by the group of S. Deki at Kobe University.<sup>11</sup> The group demonstrated that noble metals can be dispersed into low-molecular-weight nylon-11 by evaporation of a thin metallic film on the amorphous polymer, produced by vapor phase deposition and thermal crystallization of the polymer. Unfortunately, this approach does not seem to be applicable to other amorphous polymers with higher molecular weight and sluggish crystallization kinetics.

In the present paper we report the dispersion of Au into bisphenol A-polycarbonate by a new technique that has similarities to the relaxative autodispersion process. A thin film of Au is evaporated onto the amorphous polymer, and crystallization is induced at room temperature by sorption of acetone vapor which causes plasticization of the polymer matrix. While vapor sorption is a fast process, crystallization and metal dispersion take place on a much longer time scale.

## Experimental Section

Polycarbonate films with a typical thickness of 1.5–2  $\mu\text{m}$  were used in this work. The bisphenol A-polycarbonate

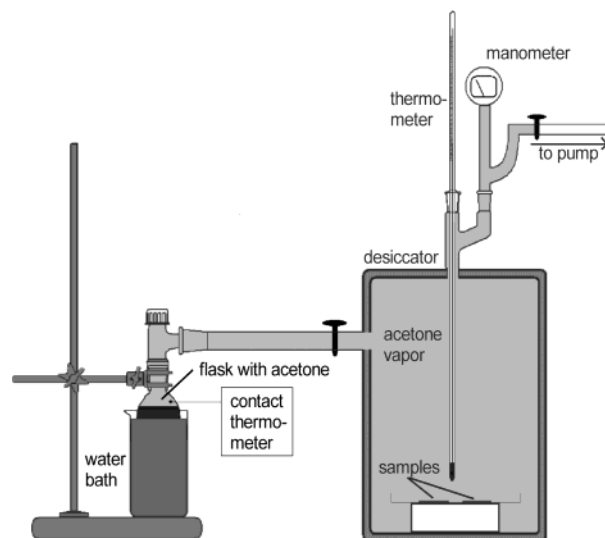


**Figure 1.** Experimental setup for the vapor-induced crystallization.

(BPA-PC;  $M_n = 14\,200$ ,  $M_w = 29\,300$  g/mol) was provided as pellets by BAYER (Leverkusen, Germany). The 0.5 wt % solution of BPA-PC was prepared by dissolving the pellets in water-free dichloromethane (DCM) in an ultrasonic bath. The solution was filtered through a Nalgene 0.2  $\mu\text{m}$  PTFE filter mounted on a glass syringe. The films were prepared by solution casting of BPA-PC in DCM on a heated (approximately 308 K) 6 in. silicon wafer placed in a Petri dish. This fast evaporation method avoids crystallization and leads to an amorphous polymer film.<sup>12</sup> The films were heated in a vacuum oven for 24 h at 353 K to remove residual DCM.

The gold was deposited on the film at 293 K by a 15 min thermal evaporation from a molybdenum crucible mounted in an ultrahigh-vacuum chamber. The deposition rate 0.1 nm/min was monitored by a quartz crystal microbalance. Thus, the total nominal gold thickness was  $\sim 1.5$  nm. The pressure did not exceed  $1 \times 10^{-7}$  Pa during the evaporation process. The metallized polymer samples were exposed to acetone vapor at a sample temperature of 303 K (Figure 1).

The desiccator was connected with a glass flask containing acetone and a membrane pump. After the desiccator was evacuated, it was flooded with acetone vapor from the flask,

<sup>†</sup> Technische Fakultät der Christian-Albrechts-Universität Kiel.

<sup>‡</sup> Kobe University.

<sup>§</sup> On leave from Silesian University of Technology, Faculty of Chemistry, Department of Physical Chemistry and Technology of Polymers, Strzody 9, PL-44100 Gliwice, Poland. Current address: University of Cambridge, Department of Materials Science and Metallurgy, Pembroke Street, Cambridge, CB2 3QZ, United Kingdom.

\* Corresponding author: e-mail ff@tf.uni-kiel.de.

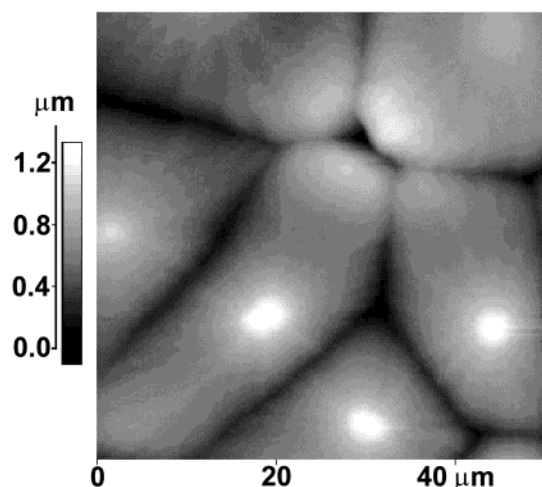


**Figure 2.** AFM micrograph of the surface of 2  $\mu\text{m}$  BPA-PC film after 10 h exposure time.

which had a temperature of 298 K to avoid condensation of acetone on the samples.

The dried samples were characterized by atomic force microscopy (AFM) ("Autoprobe cp" from Park Scientific Instruments), polarized light microscopy with direct light (PLM) (Reichert-Jung MeF3a), transmission electron microscopy (TEM) (Philips CM30), and X-ray photoemission spectroscopy (XPS) depth-profiling (Omicron Full Lab with a VG Microtech XR3E2) in conjunction with ion beam sputtering. Before sputtering, copper was evaporated onto the crystallized samples to distinguish between sputter artifacts, surface roughness, and dispersion.

Nonmetallized samples were investigated to obtain information about the crystallization process. They were characterized by infrared reflection-absorption spectroscopy (IR-RAS), X-ray diffractometry (XRD), and AFM.

## Results

Generally polycarbonates do not crystallize easily due to their stiff backbone of carbonate groups and bulky phenyl groups. Even at 458 K (36 deg above glass transition temperature ( $T_g$ )) the first indications of crystallization are detectable after  $\sim 40$ –50 h of annealing.<sup>13</sup>

However, the crystallization velocity is increased significantly by acetone vapor. The acetone vapor penetrates the BPA-PC, the polymer swells, and the chains become mobile, leading to a depression of the glass transition temperature ( $T_g$ ) below room temperature.<sup>14</sup> Whereas the sorption of a film with a thickness of  $\sim 2$   $\mu\text{m}$  is in the range of minutes,<sup>14</sup> visible crystallization occurs in a couple of hours (Figures 2 and 3).

The spherulites have diameters up to 40  $\mu\text{m}$ . A closer look shows fibril-like structures. The spherulites are quite flat. Profilometer measurements showed that their height is in the range of the film thickness ( $\sim 2$   $\mu\text{m}$ ).

AFM and PLM investigations indicated that there is no significant change in the spherulite morphology after approximately 10–30 h (Figures 2 and 3). To gain more insight into the kinetics of the crystallization process, a thin film of BPA was examined by IR-RAS and XRD.

Despite the discussion about the preferred conformation in amorphous BPA-PC,<sup>15</sup> Dybal et al.<sup>16</sup> showed that the changes in the C–O–C and the C=O stretching mode of the polycarbonate detected by IR spectroscopy (cf. Figure 4) can be easily identified with polymer crystallization independent from the discussed conformational changes.

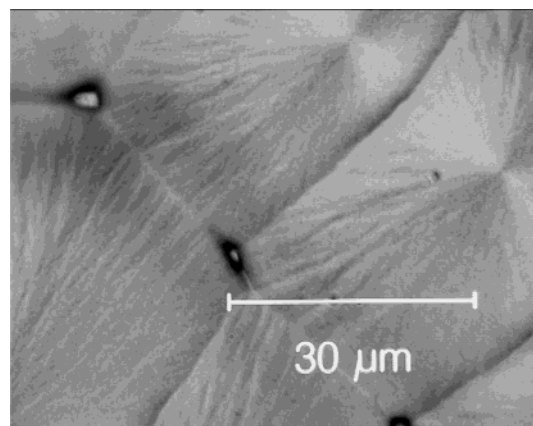


**Figure 3.** PLM micrograph of the surface of 2  $\mu\text{m}$  BPA-PC film after 35 h exposure time.

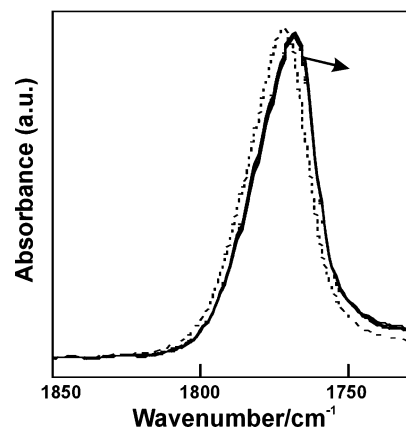


**Figure 4.** Alteration of the carbonyl stretching mode in IR spectra from amorphous (dotted line) to crystalline BPA-PC (solid line).

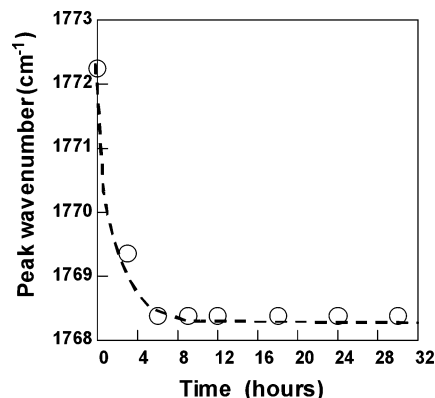


**Figure 5.** Exposure time dependence of the peak shift of the carbonyl stretching mode in IR-RAS spectra.

The shift of the corresponding peak of the C=O stretching mode in the IR spectra in Figure 5 thus indicates that the crystallization time of the nonmetallized polymer is in the range of 6–15 h, which is in good accordance with the observations by AFM and PLM.

Three samples, one amorphous, one crystallized by 17 h of acetone vapor exposure, and one well-crystallized by solvent-induced crystallization by means of dichloromethane, were investigated by XRD. One can conclude from Figure 6 that most of the crystallization process took place after 17 h of exposure.

Metallized samples surfaces, crystallized in the acetone vapor chamber for different exposure times, were

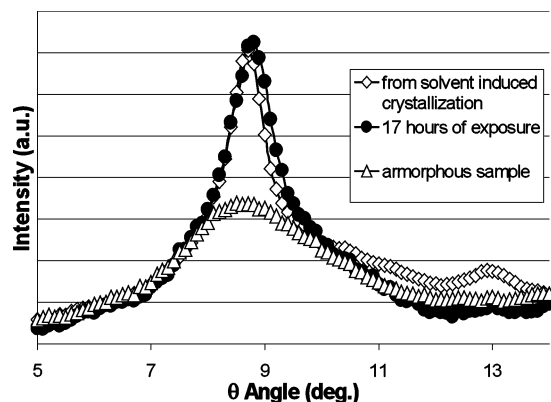


**Figure 6.** Comparison of XRD spectra of amorphous BPA-PC and crystallized BPA-PC (by solvent- and vapor-induced crystallization).

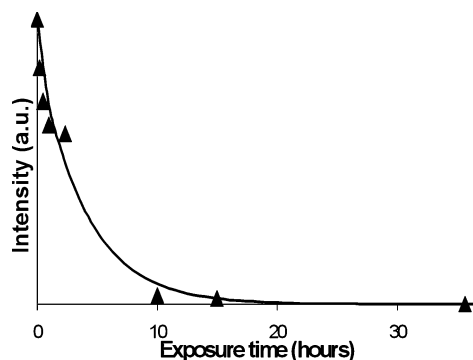


**Figure 7.** Signal of the gold 4f emission from XPS measurements on the surface of metallized and crystallized BPA-PC thin films with different exposure times to acetone vapor.

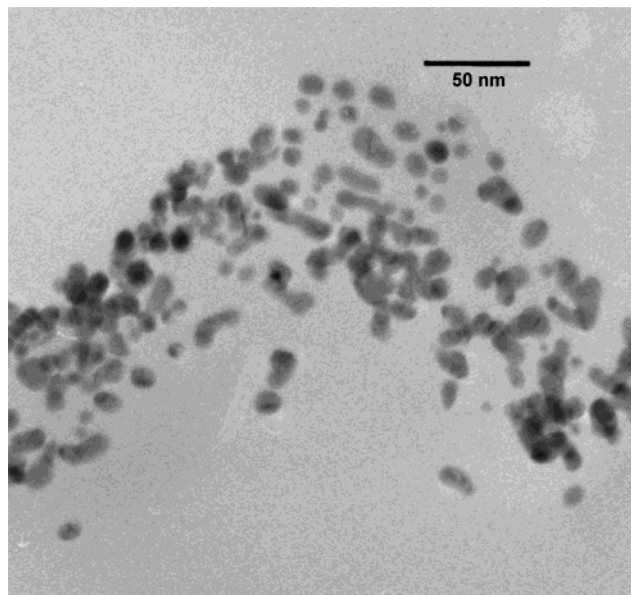


**Figure 8.** Cross-sectional TEM micrograph of dispersed gold cluster in a crystallized thin BPA-PC polymer film.

examined by XPS, which is highly surface-sensitive. It is obvious that the gold signal (4f) in Figure 7 vanished almost completely from the surface after 10–20 h of exposure time.

An average cluster size of 8–10 nm in diameter was determined from cross-sectional TEM micrographs like in Figure 8. A dispersion over a range of approximately 50–100 nm was observed, too. However, it was not

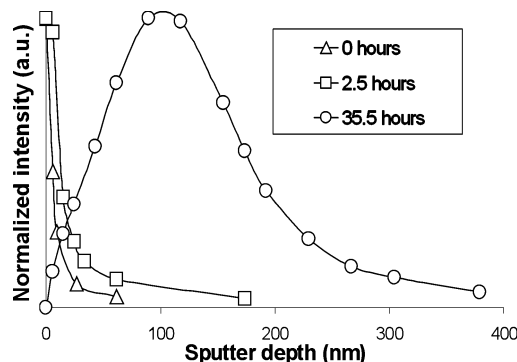


**Figure 9.** Signal of the gold 4f emission from XPS measurements after sputtering of metallized and crystallized BPA-PC thin films with different exposure times to acetone vapor (0, 2.5, 35.5 h).

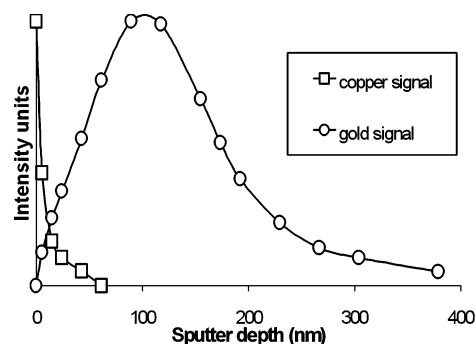


**Figure 10.** Signals of the gold 4f and the copper 2p emission from XPS measurements after sputtering of metallized and crystallized BPA-PC thin films with an exposure time of 35.5 h and metallization with copper after crystallization to determine sputter artifacts.

possible to get reliable information about the embedding depth below the surface from cross-sectional TEM.

The embedding depth for the different exposure times could be obtained by depth profiling by the means of ion beam sputtering and subsequent XPS measurement of the gold signal (4f transition) in Figures 9 and 10. Assuming a constant sputter etch rate, the sputter depth was calculated from the sputter time and the final sputter depth. The sputter depth was determined by measuring the height of a step covered by a metal sheet, using a profilometer (DEKTA 8000).

The peak width of approximately 150 nm is in the range of the result from the TEM micrograph. The comparison of the gold signal and the signal of a copper marker layer evaporated after the crystallization (Figure 10) allows to reason that the sputter depth can be identified with the embedding depth of the gold clusters with an error <20 nm.

## Discussion

When a polymer crystallizes, the crystals grow from individual nuclei. The chains fold and form lamellae with a thickness of 10–20 nm.<sup>17</sup> Usually the lamellae radiate like spokes of a wheel in three dimensions. In the present case the polymer is a thin film, so the lamellae cannot grow in every dimension uniformly. Although, because of the thin film thickness, we have more or less two-dimensional spherulites, we expect the first nuclei to form at the surface exposed to the acetone



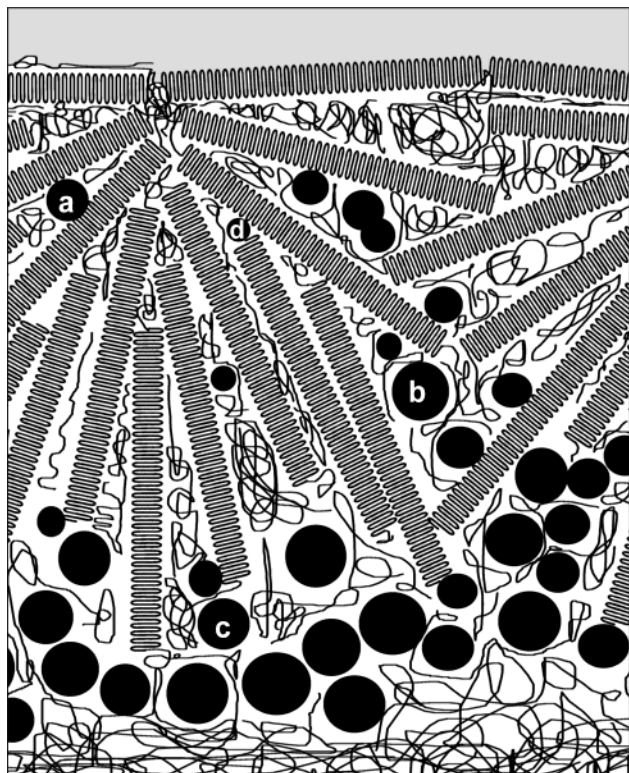


**Figure 11.** Highly schematic illustration of the dispersion model: (a) cluster trapped between branching lamellae; (b) cluster trapped between spherulites; (c) cluster in the amorphous region; (d) smaller cluster not disturbing the structure.

vapor. Hence, lamellae should primarily penetrate the polymer from the surface into the bulk. The branching lamellae give birth to daughter lamellae, if the space between them is large enough. Amorphous polycarbonate is trapped between them. The thermodynamically most unfavorable position for a gold cluster is inside of a lamella. It is very unlikely that a cluster is incorporated into the structure of the lamella because this would cause major structural disturbance.

In the amorphous area, the clusters have three possible positions in Figure 11. However, position (c) in the noncrystallized area is the most likely position; some clusters will be trapped between the spherulites (b) or between branching lamellae (a). If the crystallites grow deeper into the film, the number of such areas will rise and more clusters are trapped, so we expect the dispersion to slow down and to stop after some time. Although our results show this slowdown, we are not sure about the end of the process yet. Furthermore, smaller clusters should not be dispersed to such depths as the larger ones. They do not disturb the structure of the lamellae

as much, and they can stay in smaller amorphous regions (cf. Figure 11d).

## Conclusion

In our ongoing research we show that a layer of gold clusters on the surface of an amorphous polymer can be dispersed onto the polymer bulk by vapor-induced crystallization. Since the dispersion is on the same time scale as the crystallization process, we assume that the crystallization is the cause for the dispersion.

Our proposed model, assuming that the clusters are dispersed because of their thermodynamically unfavorable position in the crystalline area, is subject to further investigations. The kinetic and steric parameters (i.e., the influence of cluster size and exposure time) of this process are of special interest.

**Acknowledgment.** Financial support of this work by Deutsche Forschungsgemeinschaft (DFG) and Japanese Society for the Promotion of Science (JSPS) is gratefully acknowledged.

## References and Notes

- (1) Heilmann, A. *Polymer Films with Embedded Metal Nanoparticles*; Springer: Berlin, 2003; pp 149–193.
- (2) Schmid, G. *Adv. Eng. Mater.* **2001**, *3*, 737–743.
- (3) Volokitin, Y.; Sinzig, J.; de Jongh, L. J.; Schmid, G.; Vargaftik, M. N.; Moiseev, I. I. *Nature (London)* **1996**, *384*, 621–623.
- (4) Teranishi, T.; Nakata, K.; Iwamoto, M.; Miyake, M.; Toshima, N. *React. Funct. Polym.* **1998**, *37*, 111–119.
- (5) Sun, S.; Murray, C. B.; Weller, D.; Folks, L.; Moser, A. *Science* **2000**, *272*, 1989–1991.
- (6) Teranishi, T.; Kiyokawa, I.; Miyake, M. *Adv. Mater.* **10** **1998**, *8*, 597–599.
- (7) Martinu, L.; Biedermann, H.; Zemek, J. *Vacuum* **1985**, *35*, 171–176.
- (8) Behnke, K.; Strunskus, T.; Zaporotchenko, V.; Faupel, F. *Proceedings of the 3rd Int. Conf. MicroMat 2000*; Michel, B., Winkler, T., Werner, M., Fecht, H., Eds.; Verlag ddp Goldbogen: Dresden, 2000; p 1052.
- (9) Biswas, A.; Marton, Z.; Kanzow, J.; Kruse, J.; Zaporotchenko, V.; Faupel, F.; Strunskus, T. *Nano Lett.* **2003**, *3*, 69–73.
- (10) Roy, R.; Messier, R.; Cowley, J. W. *Thin Solid Films* **1981**, *79*, 207–215.
- (11) Akamatsu, K.; Deki, S. *J. Mater. Chem.* **1998**, *8*, 637–640.
- (12) Huang, D.; Yang, Y.; Zhuang, G.; Li, B. *Macromolecules* **1999**, *32*, 6675.
- (13) Alizadeh, A.; Sohn, S.; Quinn, J.; Marand, H.; Shank, L. C.; Iler, H. D. *Macromolecules* **2001**, *34*, 4068.
- (14) Ogawa, T.; Masuichi, M. *J. Appl. Polym. Sci.* **1997**, *63*, 943–949.
- (15) Tomaselli, M.; Zehnder, M. M.; Robyr, P.; Grob-Pisano, C.; Ernst, R. R.; Suter, U. W. *Macromolecules* **1997**, *30*, 3579–3583.
- (16) Dybal, J.; Schmidt, P.; Baldrian, J.; Kratochví, J. *Macromolecules* **1998**, *31*, 6611–6619.
- (17) Harron, H. R.; Pritchard, R. G.; Cope, B. C.; Goddard, D. T. *J. Polym. Sci., Part B* **1996**, *34*, 173–180.

MA035249Q